Alexandria Engineering Journal (2019) 58, 891–899

HOSTED BY

Alexandria University

Alexandria Engineering Journal

www.elsevier.com/locate/aej
www.sciencedirect.com

ORIGINAL ARTICLE

Optimization and characterization of the properties of treated avocado wood flour-linear low density polyethylene composites

Rabboni Mike Government [a,*], Okechukwu Dominic Onukwuli [a], Taofik Oladimeji Azeez [b]

[a] Department of Chemical Engineering, Nnamdi Azikiwe University, Awka, Nigeria
[b] Department of Biomedical Technology, Federal University of Technology, Owerri, Nigeria

Received 24 September 2017; revised 18 July 2019; accepted 19 August 2019
Available online 3 September 2019

KEYWORDS

Characterization;
Optimization;
Properties;
Surface modification;
SEM and FTIR

Abstract The research was carried out to investigate the optimization of surface modification for avocado wood flour (ACWF) and the characterization of the treated and untreated of avocado wood flour–linear low density polyethylene composite (ACWF-LLDPE). The variation of treated filler on the mechanical and water sorption properties was investigated. The untreated and treated ACWF-LLDPE composite was characterized using scanning electron microscopy (SEM) and Fourier transform infrared (FTIR). Central Composite design of response surface model (RSM) was used to forecast the mechanical and water sorption properties of ACWF-LLDPE composite. The properties of ACWF-LLDPE composite was statistically analysed and found to be significant. The optimal treatment was particle size of 100 mesh and filler content of 22.97%. At optimum particle size and filler content, the mechanical properties were 24.972 MPa tensile strength (TS), 6.195% elongation (E), 0.863 GPa tensile modulus (TM), 62.664 MPa flexural strength (FS), 0.809 GPa flexural modulus (FM), 699.918 Pa Brinell hardness (BH), and 91.619 kJ/m^2 impact strength (IM). The corresponding water sorption (WS) at this condition was 3.338%.

1. Introduction

Thermoplastic–organic fillers composite has been the trendiest research in the global market due to high demand on these products [1]. With respect to this development, there is a need to search for more organic fillers which can be used for the production of organic filler-thermoplastic composite for local and international marketing of these products. These fillers when totally exploited would lead to significant growth of

Abbreviations ACW, avocado wood; ACWF, avocado wood flour; ACWF-LLDPE, avocado wood flour–linear low density polyethylene composite; BH, Brinell hardness; E, elongation; FM, flexural modulus; FS, flexural strength; IM, impact strength; TM, tensile modulus; TS, tensile strength; WS, water sorption

* Corresponding author.
E-mail addresses: mike.rabboni@yahoo.com (R.M. Government), onukwuliod@yahoo.com (O.D. Onukwuli), taofikoladimeji@gmail.com (T.O. Azeez).

Peer review under responsibility of Faculty of Engineering, Alexandria University.

https://doi.org/10.1016/j.aej.2019.08.004

Nomenclature

List of symbols

σ_T	tensile strength
T_m	tensile modulus
f_m	maximum tensile force
A	cross sectional area
ep	elongation
ΔL	change in length
L	length of the sample
σ_f	flexural strength
F	applied load
d	thickness
b	width
L_s	length of support span
m	slope of the tangent to the initial line portion of the load deflection curve
E (bend)	flexural modulus
D	diameter of the steel ball
d_i	depth of indentation
IS	impact strength
E	energy at break
M	percentage of water absorbed
B_1	initial weight before soaking in water
B_2	final weight after soaking in water for time t.
BHN	Brinell hardness number

the GDP of Nigeria as a developing country and the world at large. Natural filler such as avocado wood flour (ACWF) is one of the filler that has the potential for manufacturing of various thermoplastic products. ACWF is wood filler that is present in avocado pear trees [2]. The trunk can be employed as a timber for furniture, local heating purpose, erecting building and as filler in wood-polymer composites. In the preparation of ACWF, there is the need for the chemical treatment of the filler in order to reduce the impurities present in the ACWF to achieve effective bonding between the filler and thermoplastic matrix. The major impurities are lignin, hemicelluloses, waxes material and other constituents [3]. Therefore, when these impurities are removed in the ACWF for the production of polymer-natural filler composites, the composites with exceptional mechanical properties will be produced. The some of the essential treatment process in which ACWF should undergo before it is used in production of composites are: acetylation, alkalization, silane process and use of coupling agents [4]. Out of the treatment process, alkalization, acetylation and the use of coupling agent presents the best method for treatment of ACWF. The target of combining the three treatment process is: removal of contamination in the filler, plasticization and improving the bond between the filler and the polymer matrix, respectively. Alkalization involves soaking of the filler in an alkaline solution. This leads to the upsetting of hydrogen bonding in the filler to enhance the surface roughness [5]. Acetylation is the process of the reaction of the filler with acetic acid. It decreases the hygroscopic nature of filler and increases the dimensional stability of composites [6–9]. Maleated coupling agent treatment is a process of reaction between the hydroxyl groups of the filler and the active groups of the polymer resin [10]. This results in improvement in the properties of the polymer composites [11]. In recent time, preparations of thermoplastic–natural filler composites do not involve chemical treatment of the filler which was not taken into account. Due to some abnormality in the properties of the composites being produced, these led to chemical treatment of organic fillers [12–15]. These include adequate water sorption, inappropriate sticking of the filler and polymer resin, low stress movement between the matrix and the filler, etc. [16,17]. This set back call for chemical treatment of new filler such as ACWF which the major reason it was considered in this research work. It has been reported that avocado wood tree (ACWF) is abundant in the eastern part of Nigeria. This was use in the production of polymer–filler composite with improved mechanical and water resistance properties [18,19]. Presently, there is no study on optimization and characterization of avocado wood-linear density polyethylene (ACWF-LLDPE) composite using surface modification for car mirror cover manufacturing. In this work, the gap of producing an optimum products and properties was breached using optimum materials so as to reduce cost of production and maximizing profit through chemical treatment.

2. Materials and methods

2.1. Material collection

2.1.1. Avocado wood flour (ACWF)

The avocado wood (ACW) was sourced from Trans Ekulu, Enugu State Nigera. It was sun-dried for 14 days after the extraction from its bark. The ACW was powdered and sieved to 100 to 20 mesh size.

2.1.2. Linear low density polyethylene (LLDPE)

LLDPE was sourced from petrochemical manufacture company at Port-Harcourt, Rivers State Nigeria.

2.2. Treatment of ACWF

The ACWF was immersed in solution of 6 wt% of sodium hydroxide for 16 h followed by 4% acetic acid for 1 h. The ACWF was rinsed with distilled water, filtered and sun-dried for 10 h. The treated ACWF was mixed with 5 wt% maleated polyethylene.

2.3. Composite preparations

The ACWF-LLDPE composite was molded at the Olikaeze Plastic Factory, Onitsha, Anambra State Nigeria. The treated and untreated ACWF was mixed with LLDPE by 5, 10, 15, 20, and 25% wt. The ACWF-LLDPE was compounded using injection moulding machine. The composites were cut according to ASTM standards.

2.4. Instrumental characterization for treated and untreated ACWF-LLDPE composite

The Fourier transform infrared analysis of the samples was carried out using Shimadzu Model 8400S FTIR spectrometer. The surface morphology of samples was viewed via Model PHENOM ProX scanning element microscope (SEM).

2.5. Determination of mechanical properties of composite samples

2.5.1. Determination of tensile properties of composite samples

The tensile properties were conducted at the Civil Engineering Workshop, University of Nigeria, Nsukka, Enugu State of Nigeria using universal tensometer BSS1610 model no 8889. The cross-head speed was between 10 and 100 cm/s. The sample was measured according to ASTM D638 of 3.2 mm × 19 mm × 160 mm. The ultimate tensile strength was evaluated using Eq. (1).

$$\sigma_T = \frac{f_m}{A} \tag{1}$$

where σ_T is the tensile strength, f_m is the maximum tensile force and A is the cross-sectional area of the material. The elongation was calculated using Eq. (2).

$$ep = (\Delta L)100/L \tag{2}$$

where ep is the elongation, ΔL is the change in length and L is the length of sample. The tensile modulus was calculated from the slope of stress-strain graph.

2.5.2. Determination of flexural properties

The flexural properties was analysed using the same machine for the tensile test. The dimensions of the flexural test samples were taken according to ASTM D790 at 3.2 mm × 19 mm × 300 mm. The flexural strength was evaluated using Eq. (3)

$$\sigma_f = \frac{3FL_s}{2bd^2} \tag{3}$$

where σ is the flexural strength, F is the load (force) at the fracture, d is the thickness, L_s is the length of the support span and b is the width of the sample. The flexural modulus was evaluated using Eq. (4).

$$E(bend) = \frac{{L_s}^3 m}{4bd^3} \tag{4}$$

where E (bend) is the flexural modulus and m is the slope of the initial straight-line portion of the load-deflection graph.

2.5.3. Determination of hardness properties composite sample

The test was performed according to ASTM E103 at 3.2 mm × 19 mm × 19 mm. The test was carried out with a steel bulb of 10 mm diameter to record various indentations. The Brinell hardness was calculated by applying using Eq. (5).

$$BHN = \frac{2F}{\pi D\left[D - \sqrt{D^2 - {d_i}^2}\right]} \tag{5}$$

where BHN is Brinell hardness number (Pa), D is the diameter of the steel ball (m), d is the depth of indentation (m) and F is the load (N).

2.5.4. Determination of impact properties

Simple beam Charpy impact tester machine was used to perform the test at University of Nigeria, Nsukka, Mechanical Engineering Department Workshop, Enugu State, Nigeria. The test was conducted based on ASTM D610-02M with dimension of 3.2 mm × 19 mm × 80 mm. The impact strength was evaluated using Eq. (6).

$$IS = \frac{E}{A} \tag{6}$$

where IS is the impact strength, E is the energy at break and A is the cross-sectional area of the specimen.

2.6. Water sorption test

The composite samples tested had the dimensions 3.2 mm × 19 mm × 19 mm. The samples were conditioned at 50 °C for 30 min in an oven, cooled and weighed [20]. The sample was soaked in water for 12 weeks at ambient temperature based on ASTM D96 – 06 and weighed again after the left over water on the surface was detached. The water sorption percentage was evaluated using Eq. (7).

$$M = \frac{B_2 - B_1}{B_1} \times \frac{100}{1} \tag{7}$$

where M is the percentage of water absorbed, B_1 is the initial weight and B_2 is the weight after soaking in water.

2.7. Experimental design and data analysis

Central composite design was used with particle size 100–20 mesh and filler content 5–25% as the main factor for the treated ACWF. This resulted to 13 trials for the different ACWF content and size. Design expert software version 7.0 was used for the statistical analysis, modeling and optimization. In addition, the effect of variation of treated ACWF on the composite properties was evaluated.

3. Results and discussion

3.1. FTIR analysis of treated and untreated LLDPE/ACWF composite

Figs. 1 and 2 show FTIR spectra for untreated and treated LLDPE/ACWF composite. The distinct peaks of the specimen were associated with the format in the FTIR chart [21]. In Figs. 1 and 2, the region of 3972.36 to 3325.32 cm^{-1} is characterised by the stretching of hydroxyl group of alcohol and phenol in the celllulose. The hydroxyl group stretching of carboxylic acid was observed at 3261.96 cm^{-1} and 2544.84 cm^{-1} in the filler. The peak of 2487.24 to 2140.64 cm^{-1} is characterised by phosphorus acid and ester of the hydroxyl group stretching. The stretching of N-H and hydroxyl groups of primary amide centred at 2062.92 to 2028.22 cm^{-1}. The benzene ring aromatic compounds present in lignin and hemicellulose was consigned to 1993.8 to 1719.24 cm^{-1}. The stretching C=H group of alkenes is the properties of the region in 1636.48, 1630.92 cm^{-1} and 1626.12 cm^{-1} presents in the LLDPE. The aromatic nitro compound of NO_2 asymmetric stretching is in the band of 1519.96 cm^{-1}, 1507.56 cm^{-1} and 1504.2 cm^{-1}. The C=C

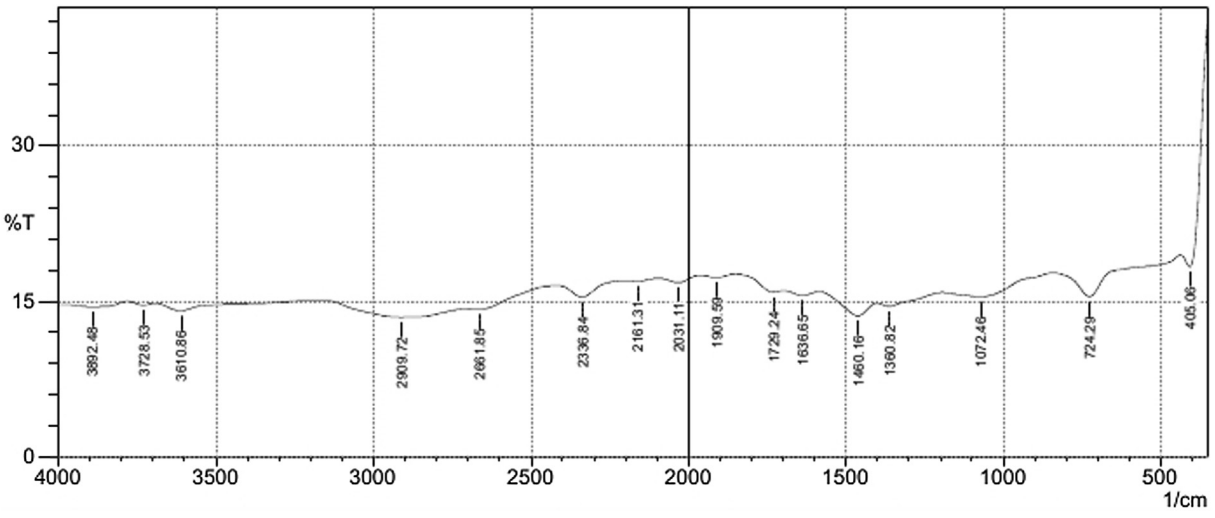

Fig. 1 FTIR for untreated LLDPE/ACWF composite.

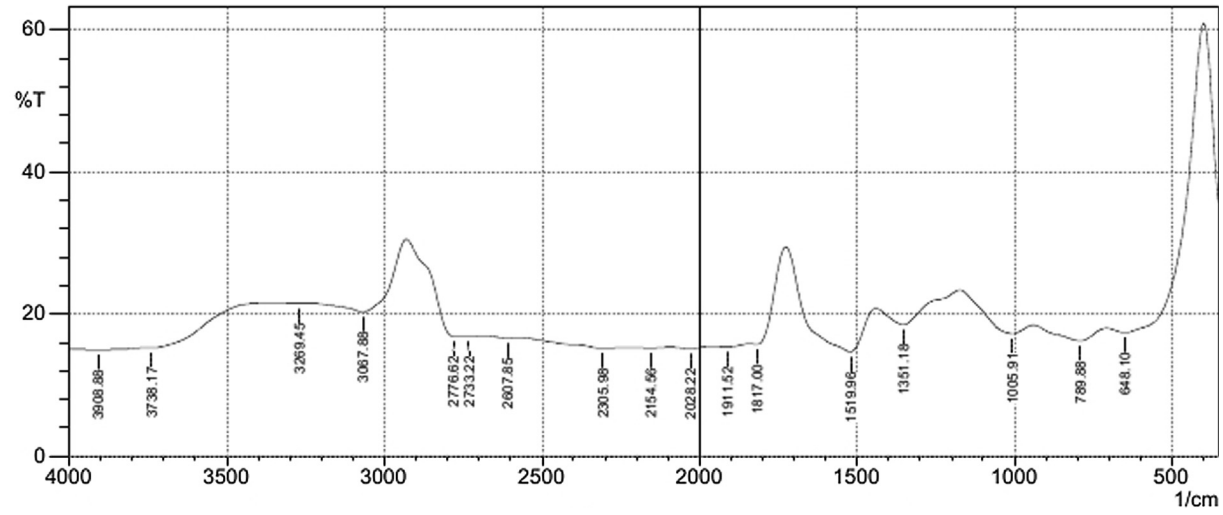

Fig. 2 FTIR for treated LLDPE/ACWF composite.

skeletal vibration stretching of aromatic disubstituted benzene is centred at 1468.68 cm^{-1} and 1460.16 cm^{-1}. The band ranges at 1442.76 cm^{-1} is allocated to N═N stretching of Azo compound. Aliphatic nitro compound of NO_2 symmetrical stretching is in the region of 1382.28 cm^{-1}. 1362.12 cm^{-1} and 1351.9 cm^{-1}. The aliphatic C—O stretching of esters is related to the region of 1259.4 to 1103.88 cm^{-1}. The region of 1074.12 to 1005.91 cm^{-1} gave the presence of C—O stretching of alcohol and phenols. The C—H bending at peaks of 982.92 cm^{-1}, 648.1 cm^{-1} and 621 cm^{-1} is a characteristic of alkenes found in LLDPE. The C—Cl stretching of alkyl halide is in the bands of 562.88 cm^{-1} to 405.06 cm^{-1}. Fig. 1 indicates the presence of aromatic compounds at 1460.16 cm^{-1} and 1360.82 cm^{-1}. This is an indication of lignin in the untreated composite. The carbonyl group near 1729.24 cm^{-1} showed the presence of hemicelluloses in the untreated filler. Figs. 1 and 2 show there is change in the position of the peak from 1519.96 to 1351.18 cm^{-1} after chemical treatment of ACWF-LLDPE composite. This is an evidence for reduction of lignin and disappearance of carbonyl group as a result of chemical treatment of ACWF.

3.2. SEM for treated and untreated ACWF-LLDPE composite

Fig. 3(a) and (b) represents SEM image for untreated and treated ACWF-LLDPE composite, respectively. Fig. 3(a) exposed white spotted ACWF particles and voids on the surface of SEM micrograph. Fig. 3(b) shows that the disappearance of the spotted particle with treated ACWF. Better wettability of fiber was observed in clearer image of SEM on Fig. 3(b) than Fig. 3(a). This is a concrete indication of a significance adhesion of ACWF and LLDPE due to chemical treatment.

Table 1 presents the design matrix of factors (particle size and filler content) and the responses mechanical and water absorption properties of LLDPE-ACWF treated composite.

Table 2 describes ANOVA analysis of the mechanical and water absorption properties of LLDPE-ACWF treated com-

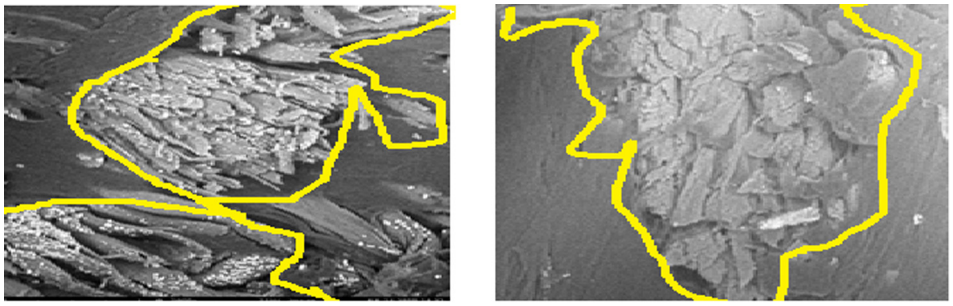

Fig. 3 SEM for (a) untreated ACWF-LLDPE composite (b) treated ACWF-LLDPE composite.

Table 1 Design matrix and response for LLDPE-ACWF treated composite in coded unit.

Run	Factors		Mechanical and water absorption properties							
	Mesh A_1	% A_2	MPa σ_T	% ep	GPa T_m	MPa σ_f	GPa E(bend)	Pa BHN	kJ/m^2 IS	% M
1	1	1	24.85	6.12	0.871	63.11	0.821	788	90.35	3.49
2	−1	1	23.13	5.72	0.837	51.96	0.77	720	66.79	3.94
3	1.267103	0	25.54	6.61	0.827	61.99	0.75	451	92.5	2.8
4	−1.2671	0	23.65	5.9	0.76	47.88	0.64	371.6	65.56	3.3
5	0	0	25.04	6.38	0.804	57.79	0.748	416	90.36	2.95
6	−1	−1	24.95	6.75	0.74	48.17	0.461	246	70.18	2.51
7	0	0	25.04	6.38	0.804	57.79	0.748	416	90.36	2.95
8	0	0	25.04	6.38	0.804	57.79	0.748	416	90.36	2.95
9	0	0	25.04	6.38	0.804	57.79	0.748	416	90.36	2.95
10	0	−1.2671	26.03	7.31	0.75	55.98	0.53	254	89.35	2.01
11	1	−1	26.3	7.21	0.783	60.52	0.627	278	93.43	2.13
12	0	1.267103	24.02	5.9	0.88	59.47	0.82	854.48	85.9	3.72
13	0	0	25.04	6.38	0.804	57.79	0.748	416	90.36	2.95

Where A_1 is the Particle Size, A_2 is the Filler Content, σ_T is the Tensile Strength, ep is the Elongation, T_m is the Tensile Modulus, σ_f is the Flexural Strength, E(bend) is the Flexural Modulus, BHN is the Brinell Hardness, IS is the Impact Strength and M is the percentage of water Sorption.

posites. It is shown that the properties (tensile strength, elongation, tensile modulus, flexural strength, flexural modulus, Brinell hardness, impact strength and water sorption, respectively, have low p value. The R^2 of the predicted model values of the properties were close to 100%. These envisaged that the model values are consistent and significant [22,23]. From the Table 2, the square of particle size (A_1^2) found to be non-significant on hardness and the filler content (A_2^2) also non-significant on σ_T and σ_f, and interactive term (A_1A_2) indicates non-significant effect on ep, T_m, IS, and M, respectively. This is as a result of p-value greater than 0.05. Eqs. (8)–(15) indicate the empirical models developed after eliminating the terms that are not significant using central composite design of experiment. The second degree models (tensile strength, elongation, tensile modulus, flexural strength, flexural modulus, hardness, impact strength and water absorption) in actual factors after eliminating insignificant terms for LLDPE-ACWF composite are:

$$\sigma_T = 24.7566 + 0.034865A_1 - 0.097335A_2 + 2.3125 \times 10^{-4}A_1A_2 + 9.31587 \times 10^{-5}A_2^2 \quad (8)$$

$$ep = 6.9444 + 0.012302A_1 - 0.094766A_2 - 4.69932 \times 10^{-5}A_1^2 + 1.42805 \times 10^{-3}A_2^2 \quad (9)$$

$$T_m = 0.6983 + 1.04703 \times 10^{-3}A_1 + 2.77553 \times 10^{-3}A_2 - 3.34489 \times 10^{-6}A_1^2 + 8.03922 \times 10^{-3}A_2^2 \quad (10)$$

$$\sigma_f = 42.12233 + 0.28888A_1 + 0.21019A_2 - 7.5 \times 10^{-4}A_1A_2 - 1.11814 \times 10^{-3}A_2^2 \quad (11)$$

$$E(bend) = 0.25188 + 4.78354 \times 10^{-3}A_1 + 0.03A_2 - 7.1875 \times 10^{-5}A_1A_2 - 2.05824 \times 10^{-5}A_1^2 - 4.53886 \times 10^{-4} \quad (12)$$

$$BHN = 231.76209 + 0.34884A_1 - 3.89818A_2 + 0.0225A_1A_2 + 0.89151A_2^2 \quad (13)$$

$$IS = 54.15239 + 0.84357A_1 + 0.49545A_2 - 4.71543 \times 10^{-3}A_1^2 - 0.021914A_2^2 \quad (14)$$

Table 2 ANOVA for the eight responses of LLDPE-ACWF treated composite: σ_T, ep, T_m, σ_f, E(bend), BHN, IS and M.

Source	Sum of squares	Df	Mean square	F Value	p-value Prob > F	Sum of squares	Df	Mean square	F Value	p-value Prob > F
σ_T						Ep				
Model	9.212848	5	1.84257	2020.813	< 0.0001	2.680981	5	0.536196	421.9177	< 0.0001
A_1	4.141436	1	4.141436	4542.063	< 0.0001	0.429386	1	0.429386	337.8716	< 0.0001
A_2	4.692219	1	4.692219	5146.127	< 0.0001	2.11641	1	2.11641	1665.343	< 0.0001
A_1 A_2	0.034225	1	0.034225	37.5358	0.0005	0.0009	1	0.0009	0.708185	0.4279
A_1^2	0.344521	1	0.344521	377.8489	< 0.0001	0.029147	1	0.029147	22.93462	0.002
A_2^2	0.000447	1	0.000447	0.490713	0.5062	0.105139	1	0.105139	82.73072	< 0.0001
Residual	0.006383	7	0.000912			0.008896	7	0.001271		
Lack of Fit	0.006383	3	0.002128			0.008896	3	0.002965		
Cor Total	9.219231	12				2.689877	12			
	R^2 = 0.999308	Adj R^2 = 0.998813		Pred R^2 = 0.99502		R^2 = 0.996693	Adj R^2 = 0.99443		Pred R^2 = 0.975439	
T_m						σ_f				
Model	0.021097	5	0.004219	189.7945	< 0.0001	270.4967	5	54.09933	1490.263	< 0.0001
A_1	0.003635	1	0.003635	163.4969	< 0.0001	237.4405	1	237.4405	6540.723	< 0.0001
A_2	0.016961	1	0.016961	762.9344	< 0.0001	16.18162	1	16.18162	445.7518	< 0.0001
A_1 A_2	2.02E−05	1	2.02E-05	0.910887	0.3717	0.36	1	0.36	9.916845	0.0162
A_1^2	0.000148	1	0.000148	6.642329	0.0366	16.50099	1	16.50099	454.5494	< 0.0001
A_2^2	0.000333	1	0.000333	14.98807	0.0061	0.013569	1	0.013569	0.373779	0.5603
Residual	0.000156	7	2.22E−05			0.254113	7	0.036302		
Lack of Fit	0.000156	3	5.19E−05			0.254113	3	0.084704		
Cor Total	0.021252	12				270.7508	12			
	R^2 = 0.992678	Adj R^2 = 0.987447		Pred R^2 = 0.945883		R^2 = 0.999061	Adj R^2 = 0.998391		Pred R^2 = 0.993028	
E(bend)						BHN				
Model	0.142206	5	0.028441	454.9447	< 0.0001	469086.8	5	93817.36	1947.95	< 0.0001
A_1	0.017613	1	0.017613	281.7346	< 0.0001	5580.78	1	5580.78	115.8749	< 0.0001
A_2	0.105074	1	0.105074	1680.768	< 0.0001	422206.2	1	422206.2	8766.359	< 0.0001
A_1 A_2	0.003306	1	0.003306	52.88683	0.0002	324	1	324	6.727282	0.0358
A_1^2	0.005591	1	0.005591	89.43778	< 0.0001	0.076696	1	0.076696	0.001592	0.9693
A_2^2	0.010621	1	0.010621	169.8961	< 0.0001	40975.73	1	40975.73	850.7879	< 0.0001
Residual	0.000438	7	6.25E−05			337.1347	7	48.1621		
Lack of Fit	0.000438	3	0.000146			337.1347	3	112.3782		
Cor Total	0.142643	12				469423.9	12			
	R^2 = 0.996932	Adj. R^2 = 0.994741		Pred R^2 = 0.977206		R^2 = 0.999282	Adj R^2 = 0.998769		Pred R^2 = 0.99475	
IS						M				
Model	1243.179	5	248.6358	332.6503	< 0.0001	3.745968	5	0.749194	831.2105	< 0.0001
A_1	908.6291	1	908.6291	1215.657	< 0.0001	0.29704	1	0.29704	329.5577	< 0.0001
A_2	16.29963	1	16.29963	21.8073	0.0023	3.407155	1	3.407155	3780.148	< 0.0001
A_1 A_2	0.024025	1	0.024025	0.032143	0.8628	0.001225	1	0.001225	1.359105	0.2819
A_1^2	293.4682	1	293.4682	392.6317	< 0.0001	0.034985	1	0.034985	38.81535	0.0004
A_2^2	24.75808	1	24.75808	33.12388	0.0007	0.005563	1	0.005563	6.172035	0.0419
Residual	5.232072	7	0.747439			0.006309	7	0.000901		
Lack of Fit	5.232072	3	1.744024			0.006309	3	0.002103		
Cor Total	1248.411	12				3.752277	12			
	R^2 = 0.995909	Adj. R^2 = 0.992815		Pred R^2 = 0.969689		R^2 = 0.998319	Adj R^2 = 0.997117		Pred R^2 = 0.987974	

A_1 and A_2 represent Particle Size and Filler Content, respectively.

$$M = 2.29104 - 0.010596A_1 + 0.081217A_2 + 5.14854 \times 10^{-5}A_1^2 - 3.28486 \times 10^{-4}A_2^2 \quad (15)$$

Fig. 4 (a–h) presents the predicted versus actual plots for the mechanical and water absorption properties of the composites. It was observed that the predicted and actual plots of all the properties of the composite converged on the diagonal line. These confirmed that the actual properties of composite were in harmony with predicted values.

Fig. 5(a–h) shows the 3D surface plots of quadratic models for the mechanical: (σ_T, ep, T_m, σ_f, E(bend), BHN, IS) and water sorption (M) properties of LLDPE-ACWF treated composite varies with particle size and filler content. The optimum properties of the composite which include tensile strength, elongation, tensile modulus, flexural strength, flexural modulus, Brinell hardness, impact strength and water absorption was depicted at Fig. 4 (a–h). It was inferred that ultimate properties of the composite at mesh particle size of 100 and filler content of 22.97 wt%.

Table 3 presents verification study of the model predicted using optimum values for the properties of LLDPE-ACWF composites. It was observed that the predicted value of the whole properties at optimum conditions depicts good agreement with experimental results. It was confirmed that from

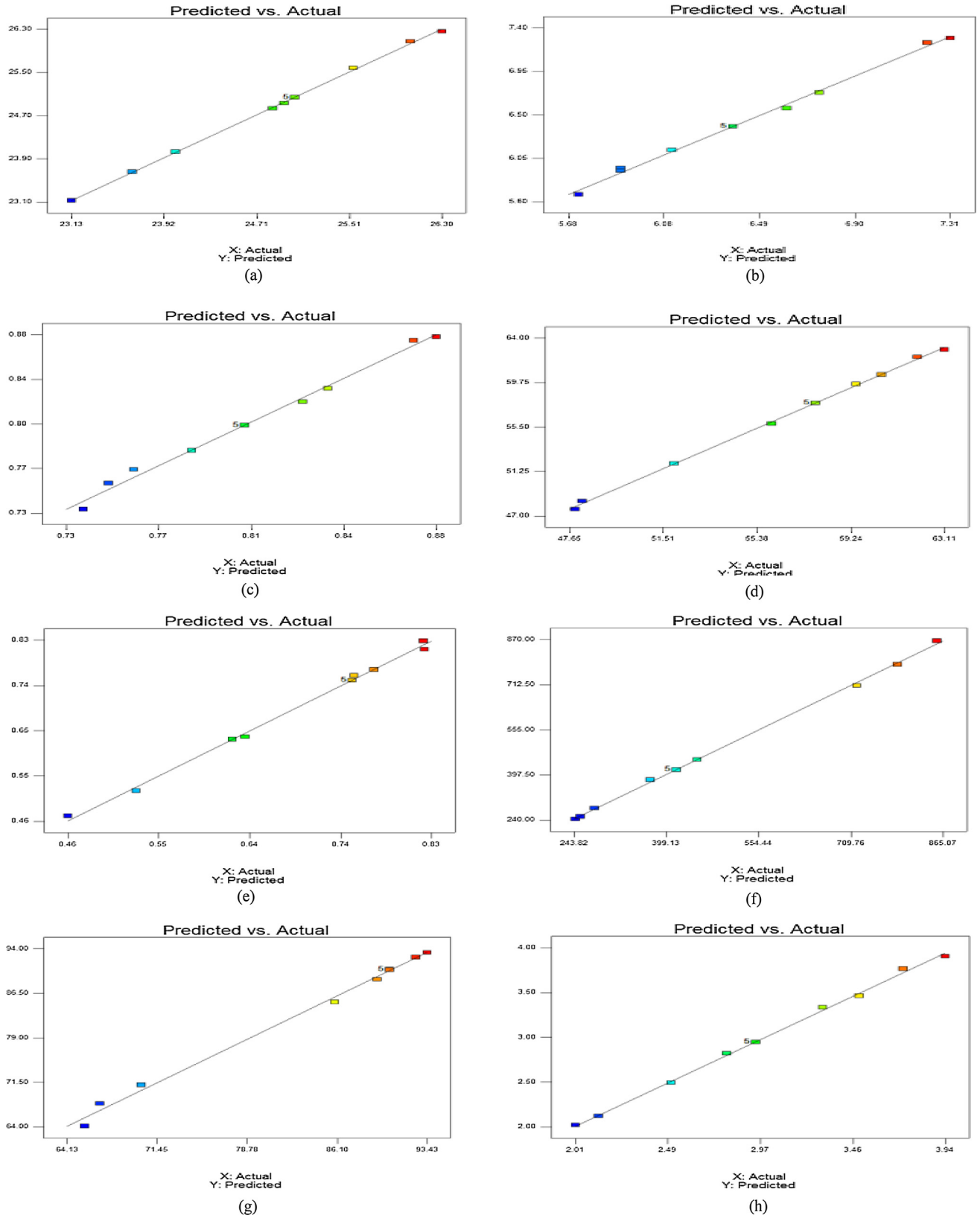

Fig. 4 Predicted vs actual plots for the mechanical and water sorption properties of LLDPE-ACWF composite: (a) σ_T (b) ep (c) T_m (d) σ_f (e) E(bend) (f) BHN (g) IS (h) M.

Table 3, the ultimate errors were very low but less than 1.5%. This shows that response surface methodology was able to forecast the experimental results very well.

More so, frequent shock load from external agents, bending effect during moulding and water absorption capability as environmental factor during washing of automobile and rain season, LLDPE/treated ACWF composite can be used in automobile side-mirror application. The properties needed for this application include tensile modulus, flexural properties, hardness, impact strength and water absorption. The

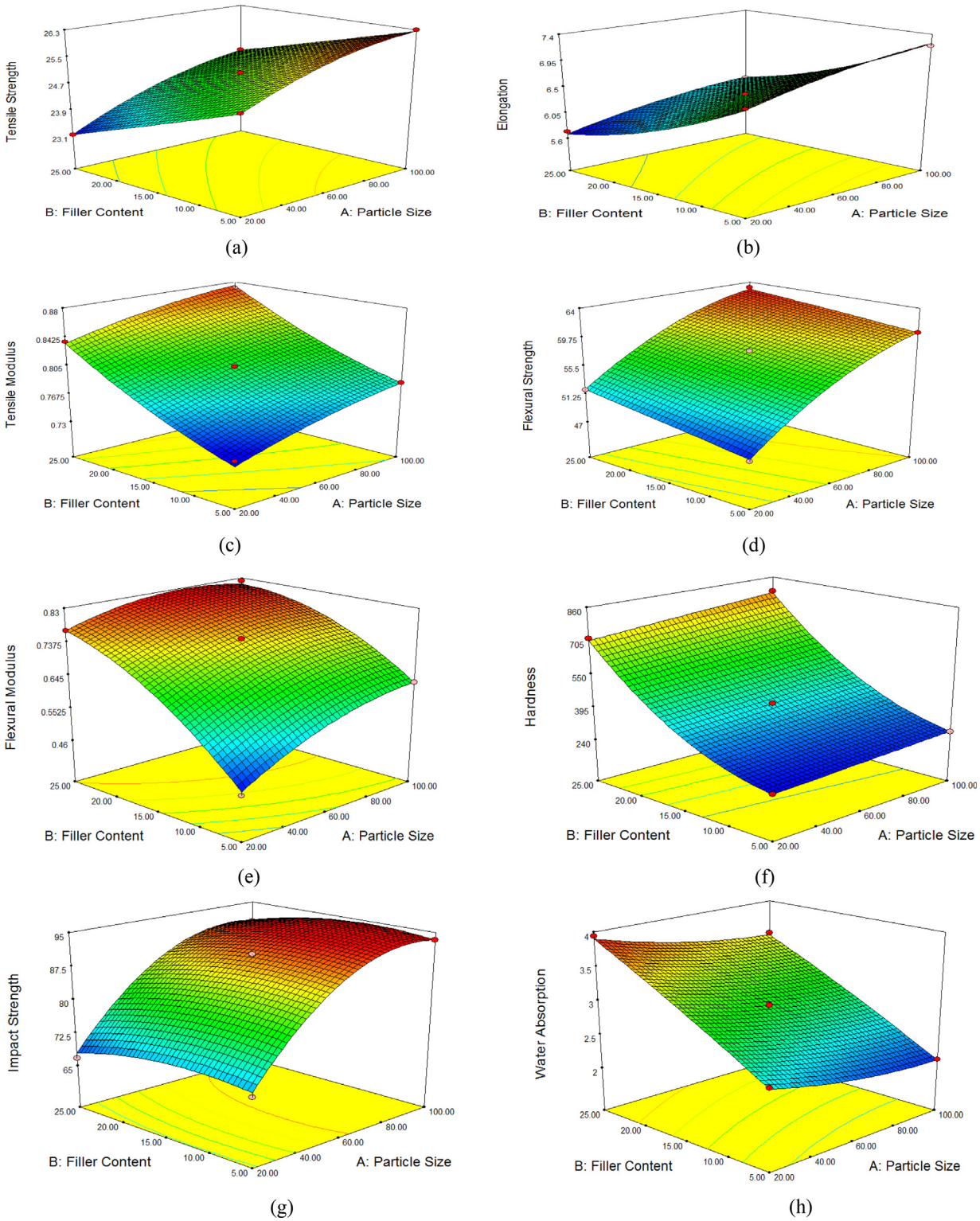

Fig. 5 3D Surface plots for the mechanical and water sorption properties of LLDPE-ACWF treated composite: (a) σ_T (b) ep (c) T_m (d) σ_f (e) E(bend) (f) BHN (g) IS (h) M varied with particle size and filler content.

Table 3 Verification study of the model predicted using optimum values for mechanical and water absorption properties of LLDPE-ACWF composites.

Properties	Particle size (mesh)	Filler content (%)	Predicted value	Experimental value	Error (%)
TS (MPa)	100	22.97	24.972	24.931	0.164445
E (%)	100	22.97	6.195234	6.145	0.817482
TM (GPa)	100	22.97	0.862804	0.857	0.677252
FS (MPa)	100	22.97	62.66374	62.395	0.430712
FM (GPa)	100	22.97	0.808934	0.799	1.243251
BH (Pa)	100	22.97	699.9178	692.288	1.102113
IM (kJ/m^2)	100	22.97	91.61887	90.372	1.379709
WS (%)	100	22.97	3.338035	3.357	0.56493

increase in properties of LLDPE/ACWF by sodium hydroxide treated ACWF commingled with 5 wt% maleated polyethylene improved the durability, flexibility, elasticity, ability to resist shock or sudden stress of LLDPE composite and hydrophilicity. Thus, sodium hydroxide treated ACWF commingled with 5 wt% maleated polyethylene enhance the quality of LLDPE composite in automobile side-mirror application.

4. Conclusion

It was shown that the optimization of properties of the ACWF varied with particle size and filler content. The characterization of the composite by FTIR and SEM analysis also described the essence of optimization of the treated composite. The optimum conditions of the factors were particle size of 100 mesh and filler content of 22.97%, while the properties of the composite at these points were 24.972 MPa of tensile strength, 6.195% of elongation, 0.863 GPa of tensile modulus, 62.664 MPa of flexural strength, 0.809 GPa of flexural modulus, 699.918 Pa of Brinell hardness, impact strength of 91.619 kJ/m^2 and 3.338% of water absorption. It is recommended that treatment of ACWF should be employed as filler for the optimization of LLDPE-composite in automobile side-mirror application.

References

[1] A.K. Bledzki, V.E. Spencer, 7th Global WPC and natural fiber composites congress and exhibition, Scientific Presentation, Kassel, Germany, 2008.

[2] K.M. Yokoyama, W. Kulavit, T. Stuart, O. Nakamoto, H.C. Bittenbender, Avocado economic fact sheet #15. Department of Agricultural and Resource Economics, CTAHR, University of Hawaii, 1991.

[3] B. Netral, T. Sabu, K.D. Chapal, A. Rameshwar, Analysis of morphology and mechanical behaviours of bamboo flour reinforced polypropylene composites, Nep. J. Sci. Technol. 13 (1) (2012) 95–100.

[4] L. Xue, G.T. Lope, P. Satyanarayan, Chemical treatment of natural fiber for use in natural fibre reinforced composites: A review, Polym. Environ. 15 (1) (2007) 25–33.

[5] A.K. Mohanty, M. Misra, L.T. Drzal, Evaluation of interface properties in fiber reinforced polymer composite using contact resonance force microscopy, Comp. Int. 8 (2001) 313–322.

[6] A.S.C. Hill, H.P.S. AbdulKhalil, M.D. Hale, A study of the potential of acetylation to improve the properties of plant fibers, Ind. Crop. Prod. 8 (1) (1998) 53–60.

[7] A. Paul, S. Joseph, S. Thomas, Effect of surface treatments on the electrical properties of low density polyethylene composites reinforced with short sisal fibers, Comp. Sci. Technol. 57 (1) (1997) 67–79.

[8] M.Z. Rong, M.Q. Zhang, Y. Liu, G.C. Yang, H.M. Zeng, The effect of fiber treatment on the mechanical properties of unidirectional sisal Reinforced epoxy composites, Comp. Sci. Technol. 61 (2001) 143–150.

[9] M.S. Sreekala, S. Thomas, Effect of fiber surface modification on the water-sorption characteristics of oil palm fiber, Appl. Comp. Mater. 5 (2003) 275–300.

[10] A.K. Bledzki, J. Gassan, Composites reinforced with cellulose based fibres, Prog. Polym. Sci 24 (2) (1999) 221–227.

[11] E. Hillig, Technical feasibility of production of composite polyethylene reinforced with wood waste and by-products of the furniture industry, Ph.D. thesis, Fede. Univ. Para., Braz., Curitiba PR, 2006.

[12] R.M. Rowell, Chemical modification of wood, In: R.W. Rowell (Ed.), handbook of wood chemistry and wood composites, Tayl. Franc. CRC Press, USA, 2005.

[13] J. Wu, D. Yu, C. Chan, J. kim, Y. Mai, Effect of fiber pretreatment condition on the interfacial strength and mechanical properties of wood fiber/pp composite, J. Appl. Polym. Sci. 76 (2000) 1000–1010.

[14] S.M.B. Nachtigall, G.S. Cerveria, S.M.L. Rosa, New polymeric-coupling agent for polypropylene/wood flour composites, Polym. Test. 26 (2007) 619–628.

[15] T.O. Azeez, O.D. Onukwuli, Properties of white roselle (*Hibiscus sabdariffa*) fibers, J. Sci. Ind. Res. 77 (9) (2018) 525–532.

[16] V. Haristov, S. Vasileva, Dynamic mechanical and thermal properties of modified polypropylene composites wood fiber composites, Macro. Mater. and Eng. 288 (2003) 798–806.

[17] A.J. Nunez, J.M. Kenny, M.M. Reboredo, M.I. Aranguren, N. E. Marcovich, Thermal and dynamic mechanical characterization of polypropylene wood flour composites, Polym. Eng. Sci. 42 (2002) 733–742.

[18] R.M. Government, O.D. Onukwuli, Effect of chemical treatment of avocado wood flour (AWF) on the properties of high density polyethylene (HDPE) for the production of natural filler composites, Int. J. Innov. Sci. Eng. Technol. 3 (2) (2016) 627–643.

[19] T.O. Azeez, O.D. Onukwuli, *Cissus populnea* fiber-unsaturated polyester composites: Mechanical properties and Interfacial adhesion, J. Nat. Fibers 15 (6) (2018) 1–14.

[20] A.G. Supri, B.Y. Lim, Effect of treated and untreated filler loading on the mechanical, morphological, and water absorption properties of water hyacinth fibre low density polyethylene composites, J. Phys Sci. 20 (2) (2009) 85–96.

[21] B. Stuart, Infrared spectroscopy: fundamentals and applications ISBNs: 0-470-85427-8 (HB): 0-470-85428-6 (PB), John Wiley. Sons, Ltd, 2004.

[22] A.I. Khuri, J.A. Cornell, Response surfaces: design and analysis, M. Dekker (Ed.), New York, 1987.

[23] K. Kuchi, Hopped delay for multiply process power control: handover procedure and optimization, Irving USA, Wile, 2000.